

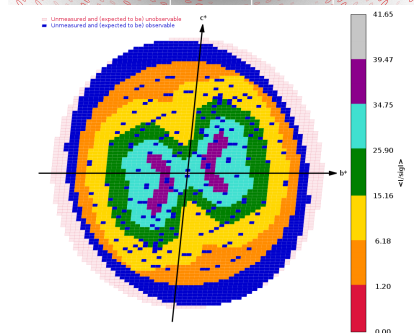
```

autoPROC 1.3.0 (20200318)
XDS VERSION Jan 31, 2020 BUILT=20200131
AIMLESS Version 0.7.4
STARANISO Version 2.3.33 (11-Apr-2020)
CCP4 Version 7.0.078
Host server8
User vonrhein (group = users)
Date Tue Apr 21 22:11:07 CEST 2020
autoPROC /home/software/xtal/GPhL/20200420
2a m1a2peg-2_#####.cbf (300 images, 150°)
3a m1a2peg-3_#####.cbf (350 images, 175°)
    
```

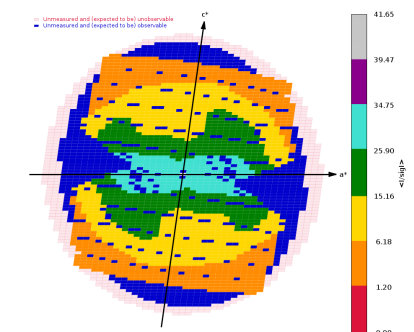
Anisotropic data analysis with STARANISO:

```

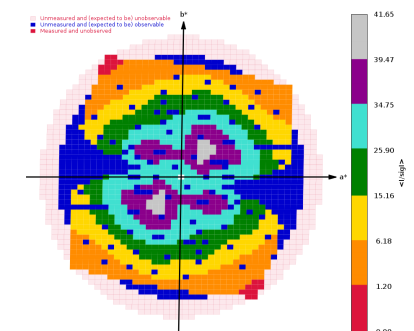
Spacegroup P1
Cell parameters 30.1468 37.7807 64.8130
                95.8014 97.9852 90.1138
Wavelength [A] 0.97918
Diffraction limits [A] 1.517 1.561 1.361
Eigenvector-1 0.942 -0.274 0.196
Eigenvector-2 0.141 0.849 0.509
Eigenvector-3 -0.306 -0.452 0.838
Direction-1 0.922 _a_* - 0.338 _b_* + 0.190 _c_*
Direction-2 0.103 _a_* + 0.776 _b_* + 0.622 _c_*
Direction-3 -0.148 _a_* - 0.274 _b_* + 0.950 _c_*
    
```



STARANISO local </sig> H=0 plane



STARANISO local </sig> K=0 plane



STARANISO local </sig> L=0 plane

	Overall	Inner Shell	Outer Shell
Low resolution limit	37.582	37.582	1.485
High resolution limit	1.361	3.749	1.361
Rmerge (all I+ & I-)	0.115	0.053	1.297
Rmeas (all I+ & I-)	0.142	0.067	1.553
Rpim (all I+ & I-)	0.082	0.040	0.845
Total number of observations	111570	6592	5173
Total number unique	37349	2535	1643
Mean(I)/sd(I)	12.5	31.8	1.4
Completeness (spherical)	61.8	88.6	11.9
Completeness (ellipsoidal)	75.2	88.6	14.2
Multiplicity	3.0	2.6	3.1
CC(1/2)	0.990	0.987	0.138
Anomalous completeness (spherical)	54.4	77.3	10.0
Anomalous completeness (ellipsoidal)	66.3	77.3	12.1
Anomalous multiplicity	1.6	1.4	1.7
CC(ano)	-0.169	-0.185	0.038
DANO /sd(DANO)	0.988	0.950	1.062

Final scaling/merging - anisotropic data analysis via STARANISO

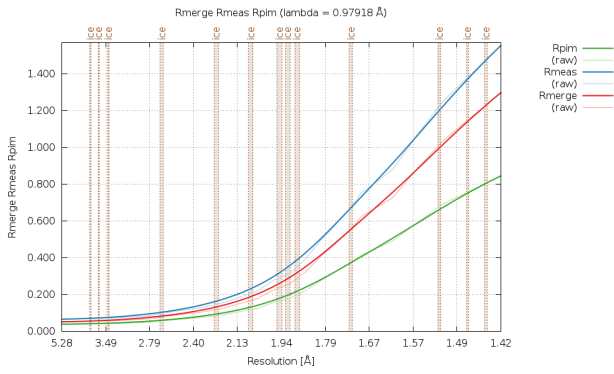


Fig.1 : R-values as a function of resolution (observations)

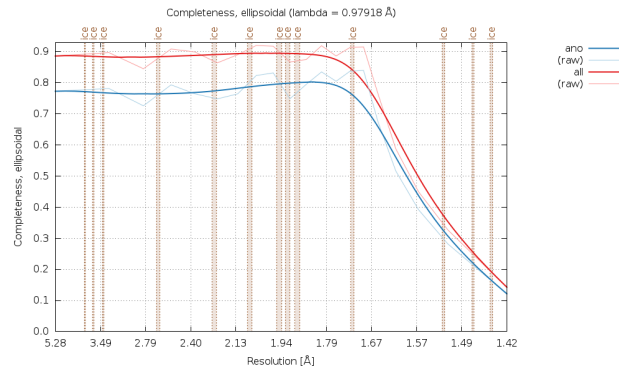


Fig.2 : Completeness (ellipsoidal) as a function of resolution (observations) - this is the relevant value here.

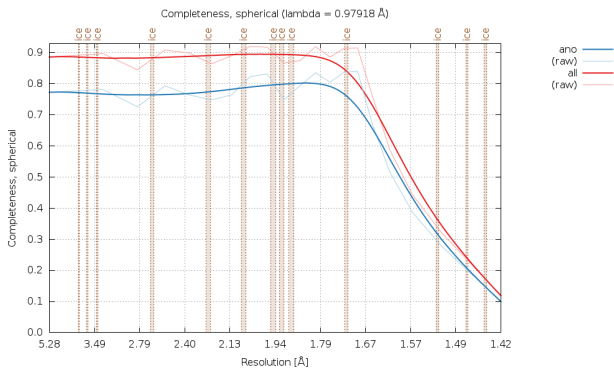


Fig.3 : Completeness (spherical) as a function of resolution (observations)

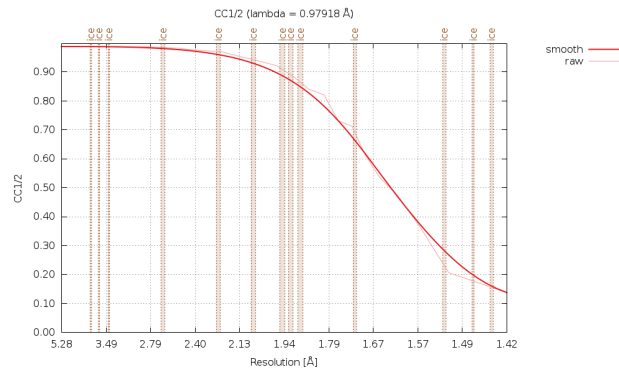


Fig.4 : CC1/2 as a function of resolution (observations)

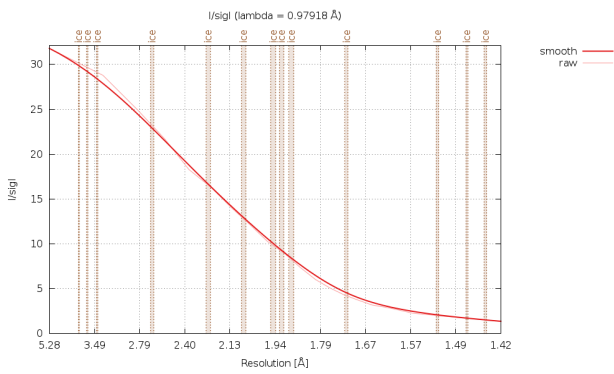


Fig.5 : I/sigI as a function of resolution (observations)

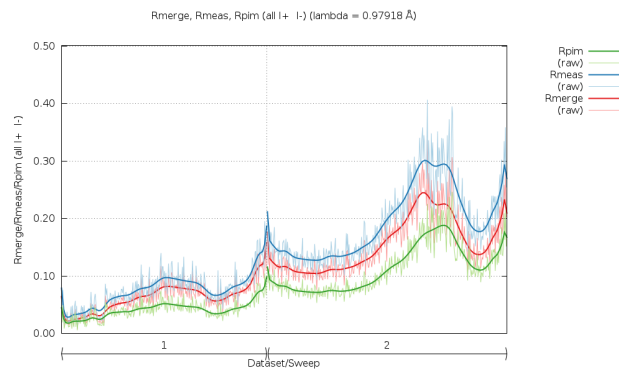


Fig.6 : R-values as a function of image number (observations)

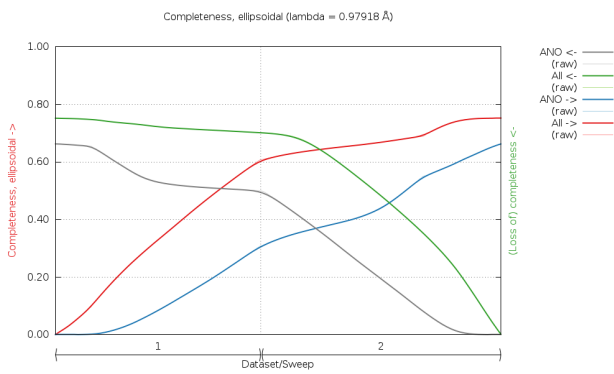


Fig.7 : Completeness (ellipsoidal) as a function of image number (observations) - this is the relevant value here.

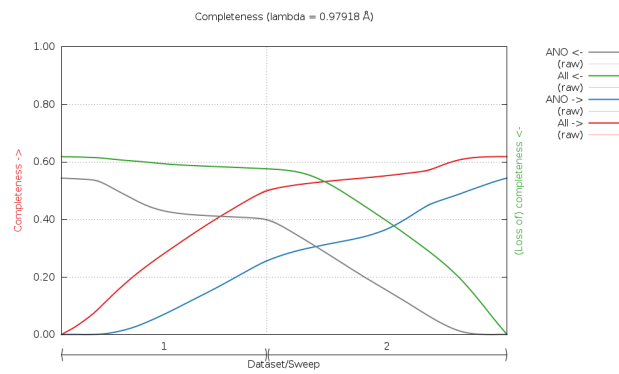


Fig.8 : Completeness (spherical) as a function of image number (observations)

Final scaling/merging - anisotropic data analysis via STARANISO

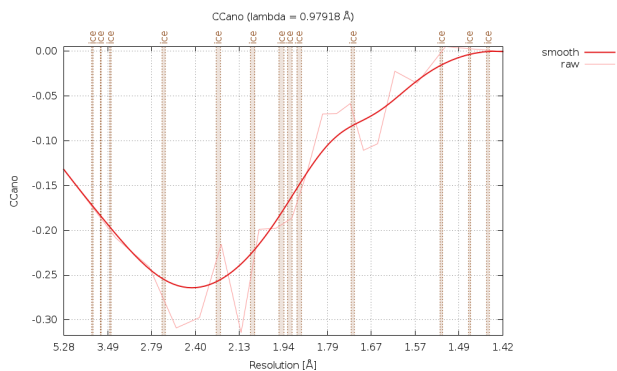


Fig.9 : CCano as a function of resolution (observations)

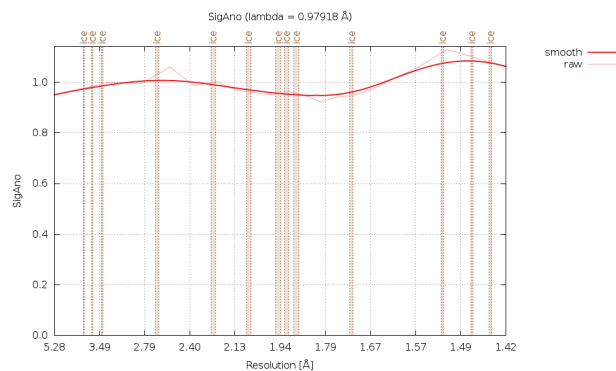


Fig.10 : SigAno as a function of resolution (observations)

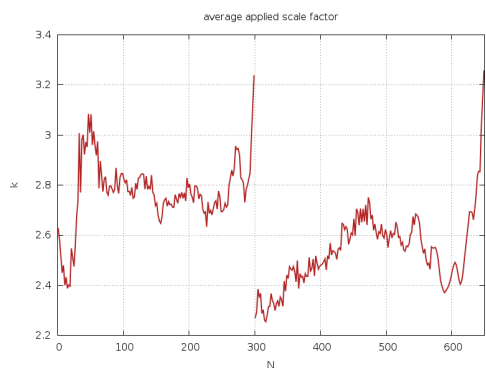


Fig.11 : Scale factor (isotropic AIMLESS scaling) as a function of image number (measurements)

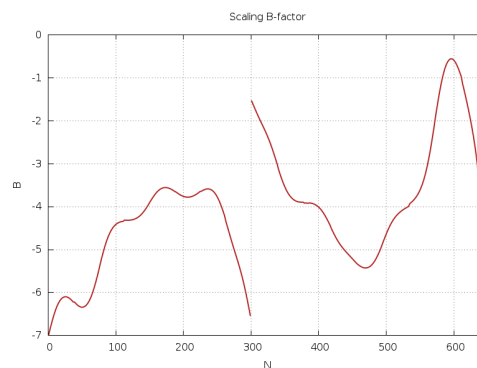


Fig.12 : Scaling B-factor (isotropic AIMLESS scaling) as a function of image number (measurements)

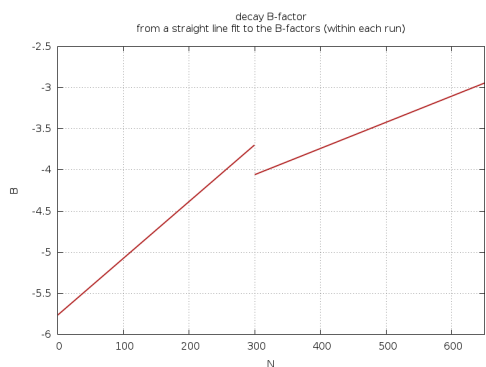


Fig.13 : Decay B-factor (isotropic AIMLESS scaling) as a function of image number (measurements)

Final scaling/merging - anisotropic data analysis via STARANISO (all measurements - for comparison only)

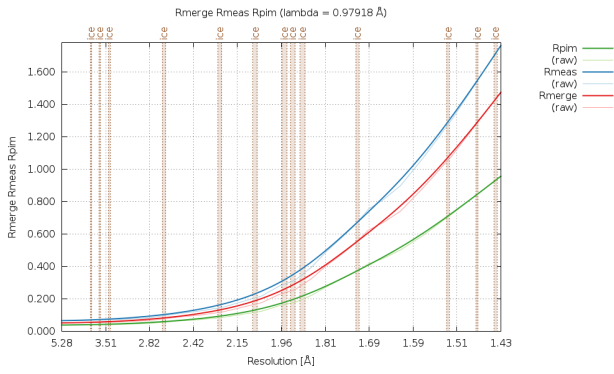


Fig.14 : R-values as a function of resolution (measurements)

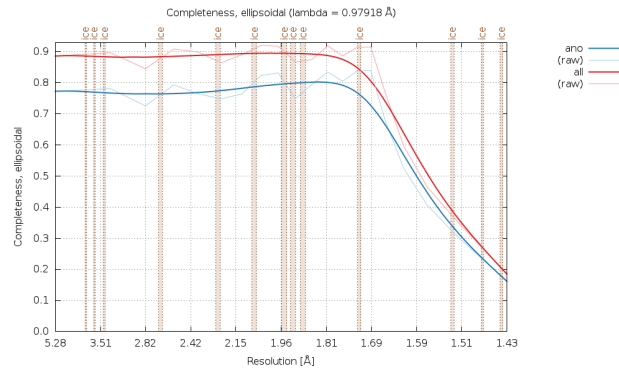


Fig.15 : Completeness (ellipsoidal) as a function of resolution (measurements)

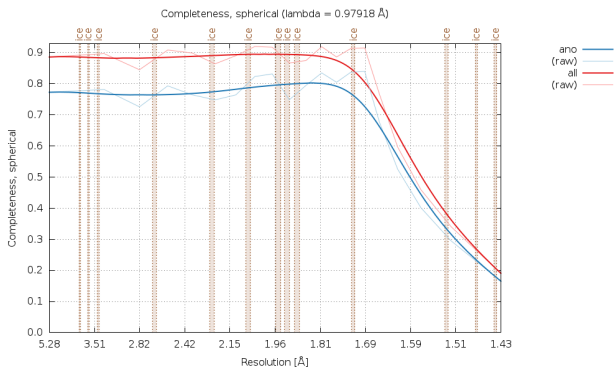


Fig.16 : Completeness (spherical) as a function of resolution (measurements)

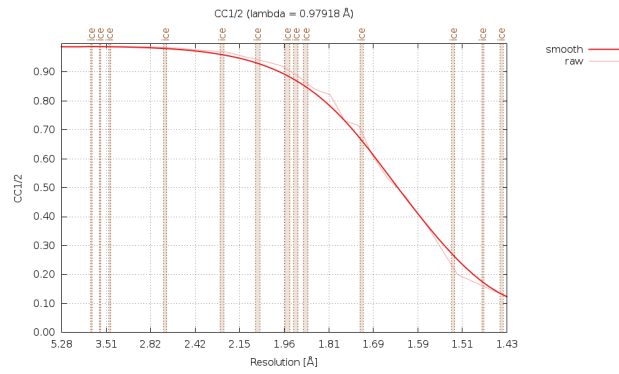


Fig.17 : CC1/2 as a function of resolution (measurements)

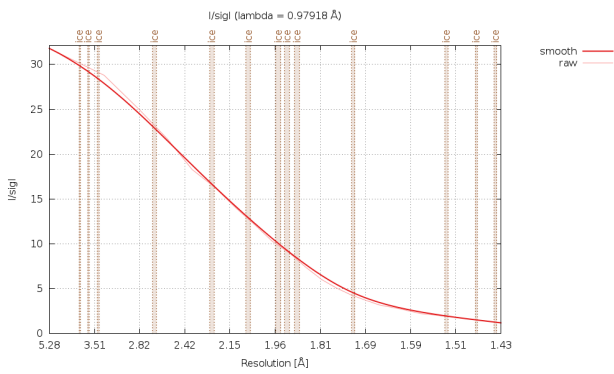


Fig.18 : I/sigI as a function of resolution (measurements)

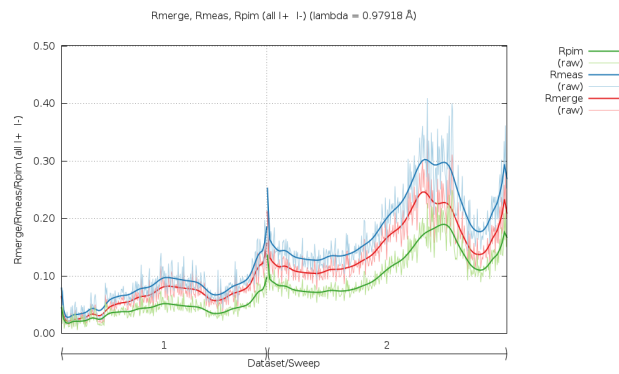


Fig.19 : R-values as a function of image number (measurements)

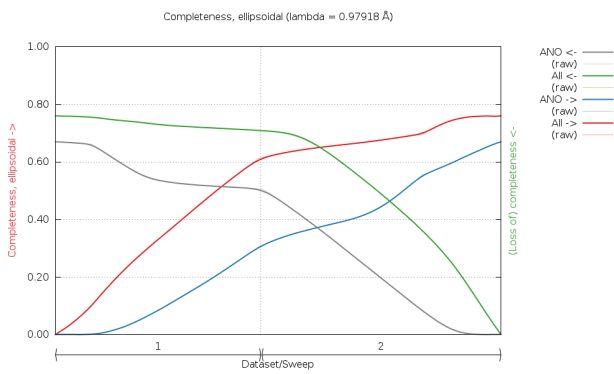


Fig.20 : Completeness (ellipsoidal) as a function of image number (measurements)

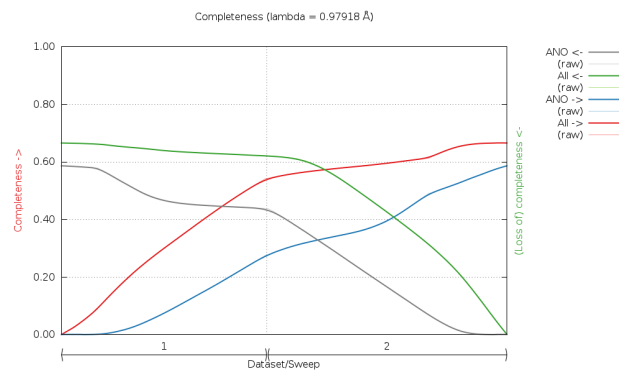


Fig.21 : Completeness (spherical) as a function of image number (measurements)

Final scaling/merging - anisotropic data analysis via STARANISO (all measurements - for comparison only)

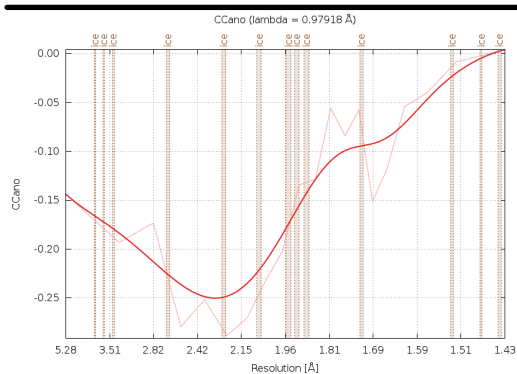


Fig.22 : CCano as a function of resolution (measurements)

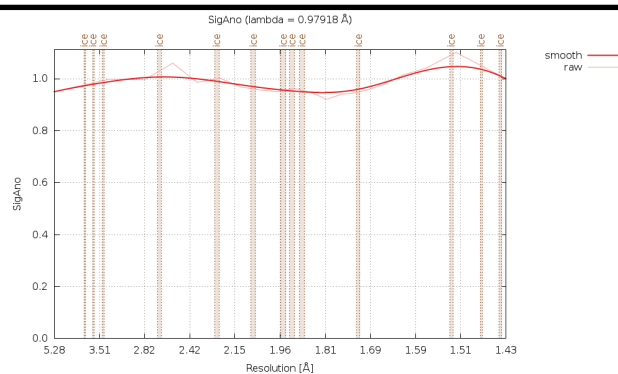


Fig.23 : SigAno as a function of resolution (measurements)

Data processing sweep 2a

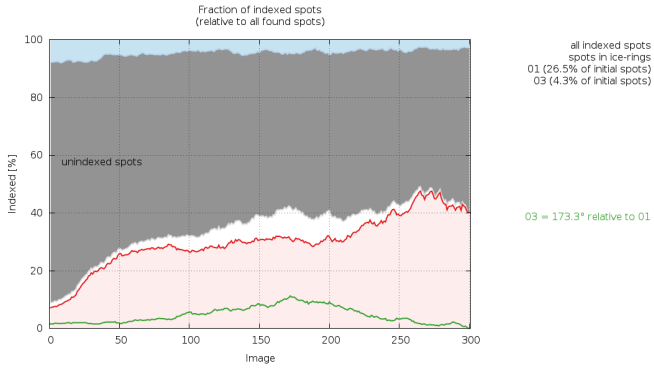


Fig.24 : (sweep 2a) number of spots for each indexing solution as a function of image number

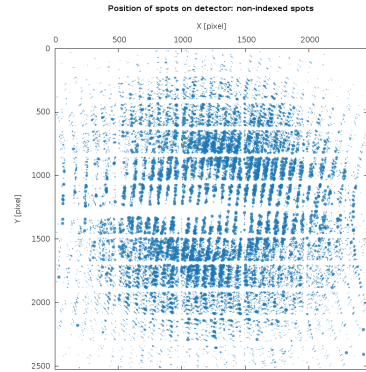


Fig.25 : (sweep 2a) unindexed spots as a function of detector position

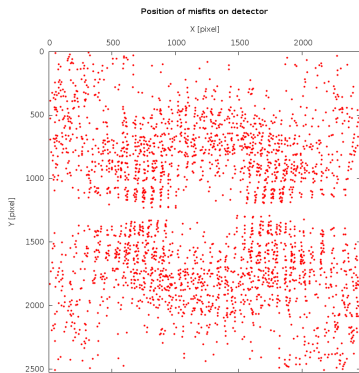


Fig.26 : (sweep 2a) reflections classified as misfits (as a function of detector position)

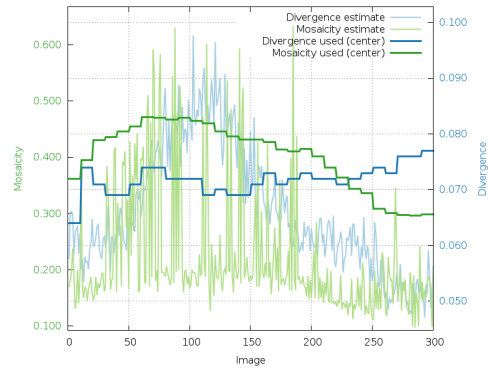


Fig.27 : (sweep 2a) divergence and mosaicity (estimated and used) as a function of image number

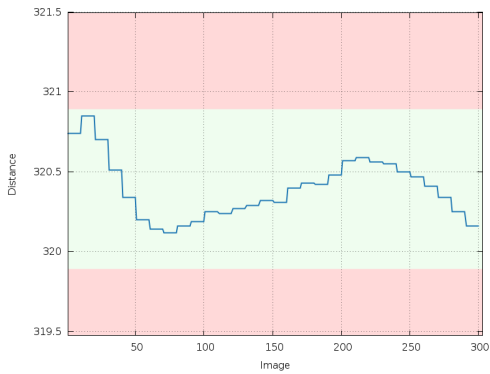


Fig.28 : (sweep 2a) refined crystal-to-detector distance as a function of image number

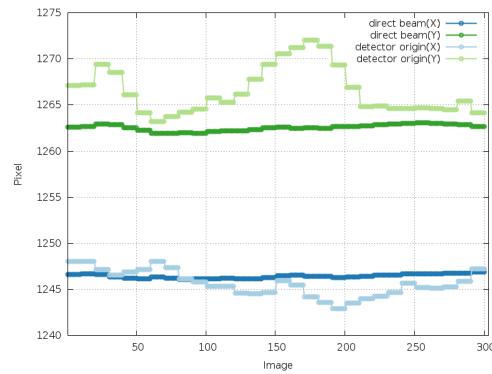


Fig.29 : (sweep 2a) direct beam position and detector origin as a function of image number

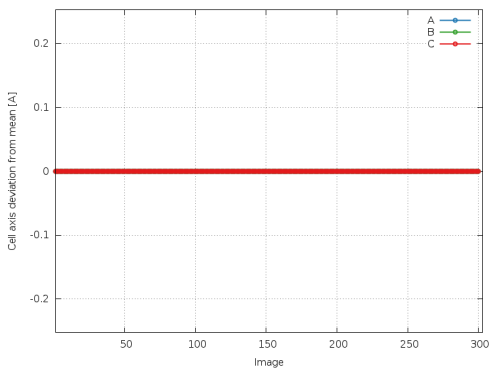


Fig.30 : (sweep 2a) deviation of refined cell axes relative to their mean (as a function of image number)

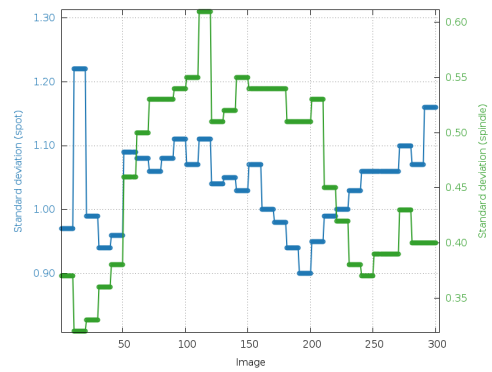


Fig.31 : (sweep 2a) standard deviation (spot position and spindle) as a function of image number

Data processing sweep 3a

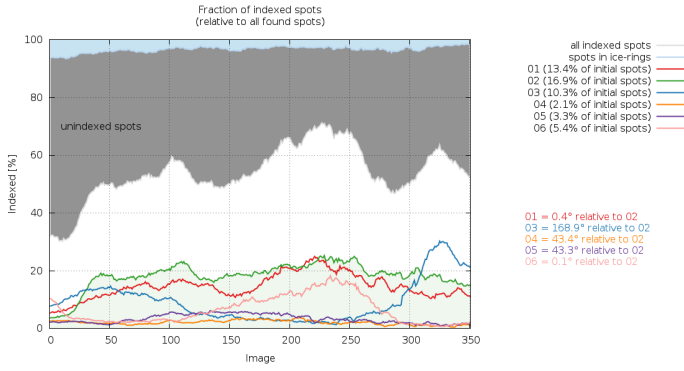


Fig.32 : (sweep 3a) number of spots for each indexing solution as a function of image number

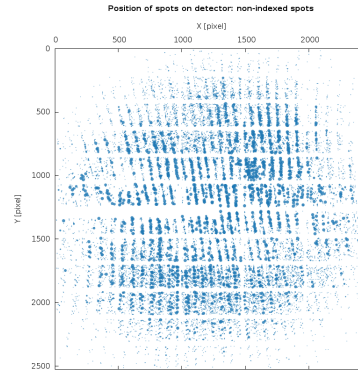


Fig.33 : (sweep 3a) unindexed spots as a function of detector position

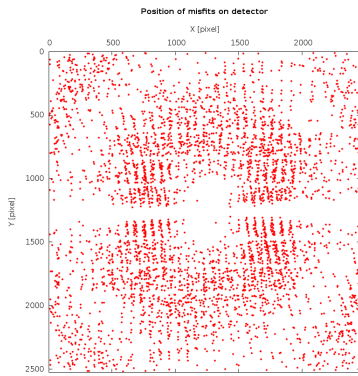


Fig.34 : (sweep 3a) reflections classified as misfits (as a function of detector position)

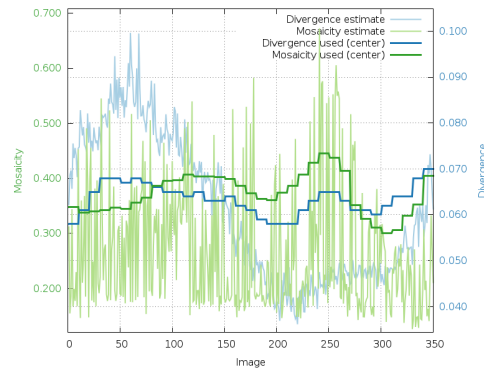


Fig.35 : (sweep 3a) divergence and mosaicity (estimated and used) as a function of image number

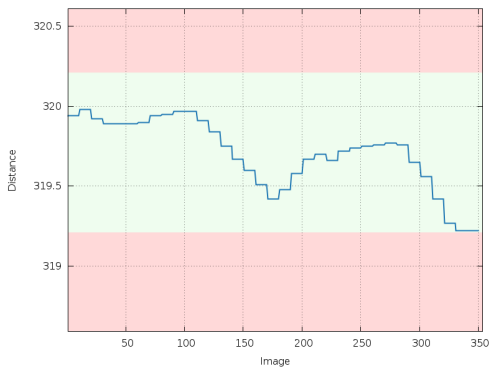


Fig.36 : (sweep 3a) refined crystal-to-detector distance as a function of image number

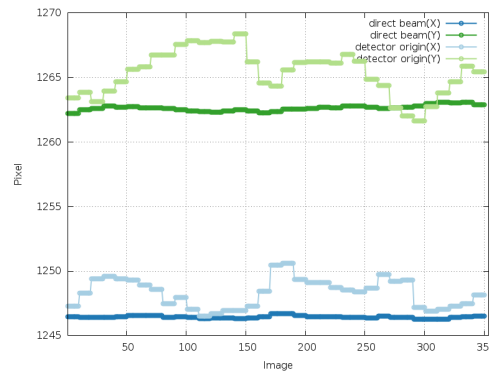


Fig.37 : (sweep 3a) direct beam position and detector origin as a function of image number

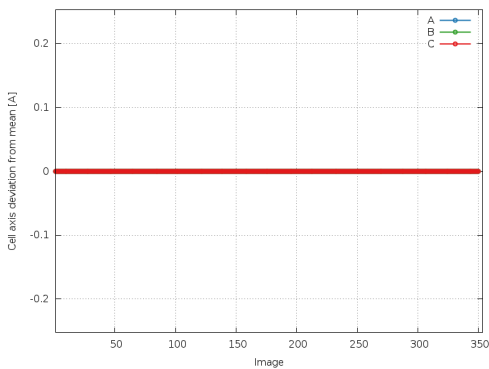


Fig.38 : (sweep 3a) deviation of refined cell axes relative to their mean (as a function of image number)

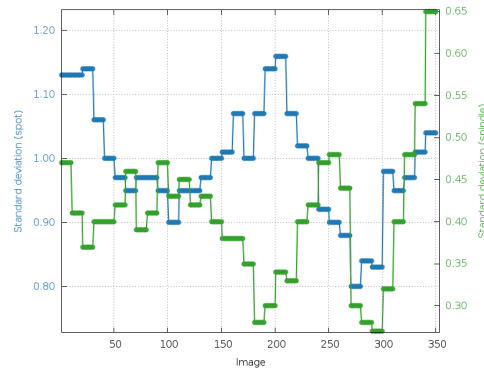


Fig.39 : (sweep 3a) standard deviation (spot position and spindle) as a function of image number

References

- autoPROC Vonrhein, C., Flensburg, C., Keller, P., Sharff, A., Smart, O., Paciorek, W., Womack, T. and Bricogne, G. (2011). Data processing and analysis with the autoPROC toolbox. *Acta Cryst.* D67, 293-302.
- XDS Kabsch, W. (2010). XDS. *Acta Cryst.* D66, 125-132.
- POINTLESS Evans, P.R. (2006). Scaling and assessment of data quality, *Acta Cryst.* D62, 72-82.
- AIMLESS Evans, P.R. and Murshudov, G.N. (2013). How good are my data and what is the resolution?, *Acta Cryst.* D69, 1204-1214.
- CCP4 Winn, M.D., Ballard, C.C., Cowtan, K.D. Dodson, E.J., Emsley, P., Evans, P.R., Keegan, R.M., Krissinel, E.B., Leslie, A.G.W., McCoy, A., McNicholas, S.J., Murshudov, G.N., Pannu, N.S., Potterton, E.A., Powell, H.R., Read, R.J., Vagin, A. and Wilson, K.S. (2011). Overview of the CCP4 suite and current developments, *Acta. Cryst.* D67, 235-242.
- STARANISO Tickle, I.J., Flensburg, C., Keller, P., Paciorek, W., Sharff, A., Vonrhein, C., and Bricogne, G. (2020). STARANISO. Cambridge, United Kingdom: Global Phasing Ltd.